EVS29 Symposium
Montréal, Québec, Canada, June 19 - 22, 2016

Sensorless Vehicle Detection Using Voltage Pulses in Dynamic Wireless Power Transfer System

Daita Kobayashi[1], Katsuhiro Hata[1], Takehiro Imura[1], Hiroshi Fujimoto[1], Yoichi Hori[1]
The University of Tokyo, 5-1-5, Kashiwanoha, Kashiwa, Chiba, 277-8561, Japan
[1]*kobayashi14@hflab.k.u-tokyo.ac.jp*

Abstract

A large amount of power loss due to power transmission while a receiving coil is not near a transmitter can be a main issue in dynamic wireless power transfer system for electric vehicles. In conventional researches, additional vehicle detection system using loop coils or other sensors has been a solution for the problem by detecting the approach of vehicles. However, additional sensors can increase troubles of installation and malfunction. Therefore, a new vehicle detection method which uses a transmitting coil itself as a sensor is proposed. The effectiveness of the proposed system is verified by experiments.

Keywords: wireless charging, dynamic charging ,EV (electric vehicle), efficiency

1 Introduction

Recently, wireless power transfer (WPT) technology via magnetic resonance coupling has been attracting attention[1]. Especially, applications for electric vehicles (EVs) are expected to be new charging methods for EVs. Moreover, dynamic wireless power transfer (DWPT) system is recently focused on as well as static wireless power transfer system that a lot of research has been carried out on. The major concept of DWPT system is transferring power from a transmitting coil buried under a road to a receiving coil attached on the bottom of EVs using magnetic resonance coupling method while EVs are cruising[2]. With this technology, Conventional short cruising range of EVs can be extended without carrying a large amount of heavy and bulky batteries. Major research subjects are the shape of coils[3], circuit topology[4], the control of power converters and so on. A DWPT system in which high power and efficient transmission is possible has been pursued by optimizing these parameters.
However, a precise vehicle detection system is also an important issue and necessary in a DWPT system since power transmission has to be carried on only while a vehicle is exactly above a transmitter to prevent large energy loss. In conventional research, loop coils or other sensors have been used for vehicle detection[5]. Yet, additional sensors can cause more troubles of installation and malfunction. Therefore, a new vehicle detection method which uses a transmitting coil itself as a sensor is proposed in this paper.

2 Wireless Power Transfer for Electric Vehicles

2.1 Magnetic Resonance Coupling

Conventionally, a few cm of power transmission was possible using electromagnetic induction. Yet, there were limited applications due to its short transmitting range. However, Researchers from Massachusetts Institute of Technology (MIT) proposed a WPT method via magnetic resonance coupling[6]. In this technology, a few meters of power transmission with higher efficiency is possible by combining LC

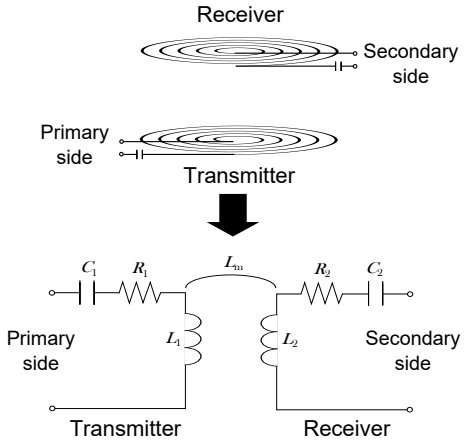

Figure 1: Equivalent circuit of magnetic resonance coupling

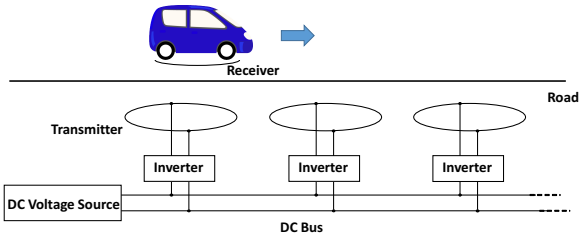

Figure 2: Proposed transmitting side (DC bus system).

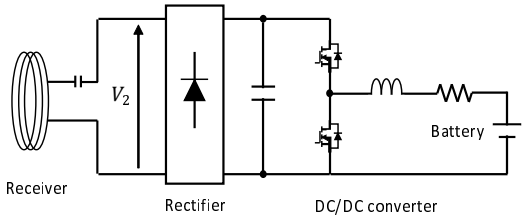

Figure 3: Receiving side

resonance and electromagnetic induction method[7]. Therefore, magnetic resonance coupling can be an appropriate method for DWPT system because of the characteristic which is highly tolerant about misalignment. Figure 1 illustrates an equivalent circuit of magnetic resonance coupling.

2.2 Transmitting-side System

Figure 2 shows a considered design of a transmitting side of DWPT which is called “DC bus system”[8]. A transmitter consists of just one series-compensated transmitting coil and an inverter controlled in constant voltage. A DC bus is laid below and each transmitter is connected to it in parallel. This simple structure makes maintenance and placement easy. In addition, high power transfer is possible because each inverter bears power for just one transmitter coil. Furthermore, the DC bus reduces EMI compared to a long AC bus.

2.3 Receiving-side System

Figure 3 illustrates a considered structure of a receiving side. The receiving side is composed of a series-compensated receiving coil, a rectifier, a DC-DC converter and a storage such as battery or super capacitor. The DC-DC converter is installed to arbitrarily change the secondary voltage V_2 in order to control the transmitting efficiency[9].

3 Sensorless Transmitting ON/OFF Switching System

In contrast to a static wireless power transfer system, it is easily possible that no vehicle is above a transmitting coil during transmission in DWPT system. However, huge current which will be only loss flows in a transmitting coil if no vehicle is on the transmitter in a system such as Figure 2. That is because impedance seen from an inverter becomes extremely low if no receiving coil is near a transmitter and low impedance for constant voltage source let huge current flows in a circuit. Conventional solutions for this problem are constant current control of an inverter[10], use of LCL circuit that converts constant voltage characteristic to constant current characteristic[11]. Nevertheless, these solution are contrary to

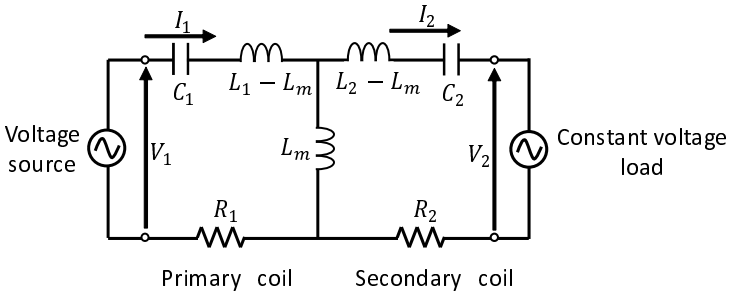

Figure 4: Simplified equivalent circuit

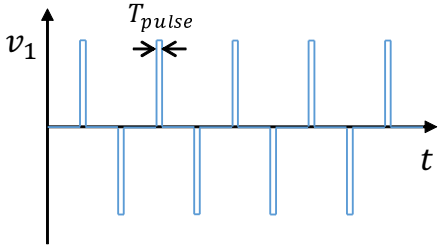

Figure 5: Searching pulse(at resonant frequency)

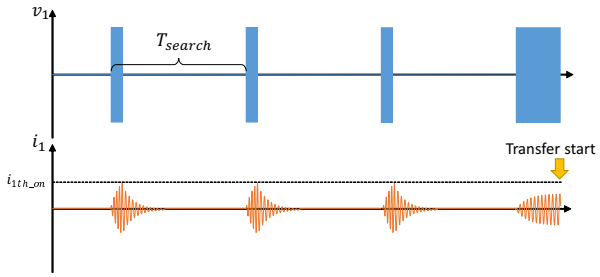

Figure 6: Searching pulse and primary current

an idea that transmitting system should be simple. Moreover, constant current causes constant copper loss in a transmitting coil. Therefore, a transmitting system which transfers power only while a receiving coil is close to a transmitting coil is ideal. Consequently, precise vehicle detection system is necessary for DWPT system.
Other research institutes proposed several vehicle detection systems which utilize additional sensors [5, 12]. However, additional sensors are able to cause more complexity and troubles of malfunction and maintenance.

3.1 Idea of Vehicle Detection

In WPT circuit using magnetic resonance coupling, secondary (induced) voltage and current have 90° of phase delay to primary voltage. With this fact, simplified WPT circuit can be depicted as a model with a constant voltage source on the secondary side (Figure 4)[13]. Furthermore, KVL equation of this model is expressed as follows.

$$\begin{bmatrix} V_1 \\ jV_2 \end{bmatrix} = \begin{bmatrix} R_1 & -j\omega_0 k\sqrt{L_1 L_2} \\ j\omega_0 k\sqrt{L_1 L_2} & -R_2 \end{bmatrix} \begin{bmatrix} I_1 \\ jI_2 \end{bmatrix} \tag{1}$$

Where, ω_0 is resonant frequency, k is coupling coefficient. From (1), primary current I_1 is derived as follows.

$$I_1 = \frac{R_2 V_1 + \omega_0 k\sqrt{L_1 L_2} V_2}{R_1 R_2 + \omega_0^2 k^2 L_1 L_2} \tag{2}$$

From (2), the smaller k a system has, the larger I_1 becomes. The main idea of the proposed method is sensing the presence of vehicle with the change in I_1 when searching voltage pulses are applied.

3.2 Searching Voltage Pulses

The image of searching voltage pulses is described in Figure 5. To reduce standby power consumption, the searching pulses are narrowed as much as possible with phase shift method of inverter. The pulse width is defined as T_{pulse}. Furthermore, the bundles of voltage pulses are applied intermittently because the voltage pulses do not need to be applied constantly. The interval between pulse bundles is defined as T_{search}. When k is large (a vehicle is near a transmitter), the envelop of the primary current I_{1env} settles at smaller value from (2). On the other hand, it becomes larger when k is small or 0. Therefore,

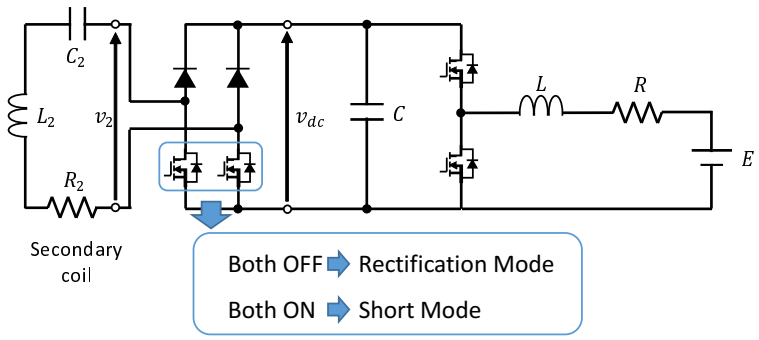

Figure 7: Receiving circuit with HAR

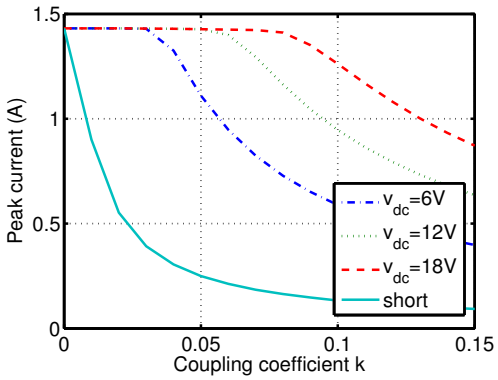

Figure 8: Comparison of primary current peak value

the presence of vehicle is judged by weather the primary current exceeds a threshold current $I_{1env\_th\_on}$ or not(Figure 6). The procedure of the searching method is below.

1. Bundles of searching voltages are applied in an interval T_{search}.
2. If I_{1env} exceeds $I_{1env\_th\_on}$, searching is stopped immediately and waits until the next period.
3. Power transfer starts if I_{1env} does not exceed $I_{1env\_th\_on}$ for certain period during the searching.

3.3 Standby Method of the Secondary Circuit

From (2), the primary current I_1 changes also depending on the secondary voltage V_2. This means that generalized current threshold $I_{1env\_th\_on}$ cannot be determined since I_{1env} can be changed by the secondary battery voltage. Therefore, the circuit illustrated in Figure 7 is proposed. This circuit is called Half Active Rectifier (HAR). In HAR, the lower diodes are replaced for MOSFETs. Thus, the secondary coil can be shorted ($V_2 = 0$) by turning ON these MOSFETs(Short mode). Therefore, the primary current does not depend on V_2 and generalized $I_{1env\_th\_on}$ can be determined by using short mode.
Here, Figure 8 shows the changes in peak values of I_{1env} at different coupling coefficient k when constant voltage pulses are applied to systems. Dotted lines illustrate the cases of rectification mode standby with several DC-link voltages v_{dc}, and a lightblue solid line shows the case of short mode standby. From Figure 8, the peak values of I_{1env} differ at the same coupling coefficient k even if v_{dc} is different with rectification mode standby. On the other hand, the peak values of I_{env} is always unity in the case of short mode standby.

3.4 Stop Method of Power Transfer

In this section, stop method of power transmission when a vehicle goes away from a transmitter is explained.
When power transfer is stopped, I_{1env} can be used in the same way as when starting the transfer. However, a more adaptive system is able to be built if the stop timing is determined by the secondary side. For instance, when battery was almost empty, a user want to receive the power as long as possible. On the

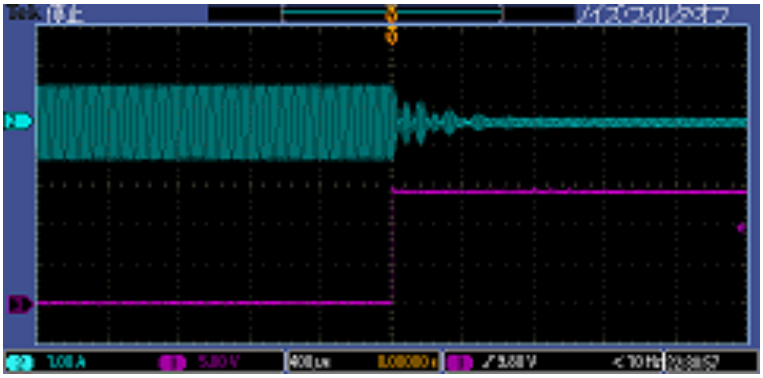

Figure 9: The primary current at short mode entry

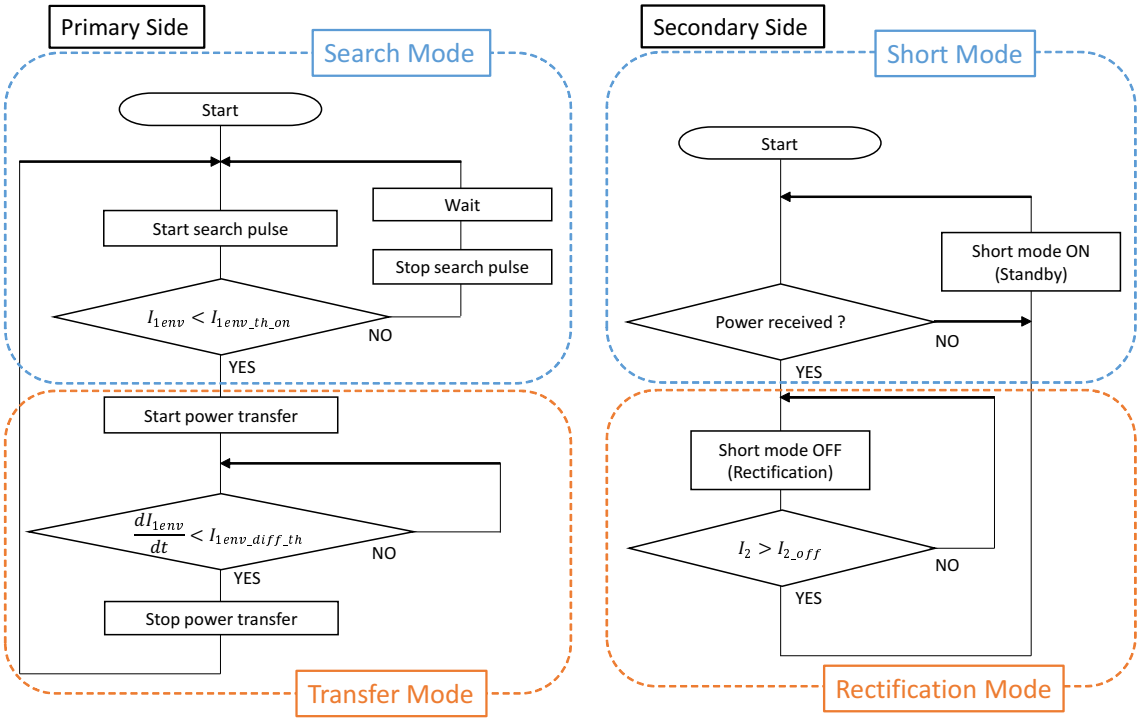

Figure 10: Flowchart of the proposed algorithm

other hand, a user who has a full battery just want to receive the power only while transmitting efficiency is high.

3.4.1 Change in the Primary Current by Short Mode

According to the discussion in the last section, the primary current I_1 changes depending on V_2. Figure 9 shows the primary current (blue line) when the secondary HAR turns into short mode. The figure indicates that the I_{1env} suddenly decreases right after short mode starts. Thus, the secondary circuit is able to send a "stop signal" to the primary side by starting short mode during power transfer and the primary circuit can receive the signal by observing the differential value of the primary current envelop $\frac{dI_{1env}}{dt}$. In particular, the primary side stops the power transfer when $\frac{dI_{1env}}{dt}$ falls below a certain threshold value $I_{1env\_diff\_th}$.

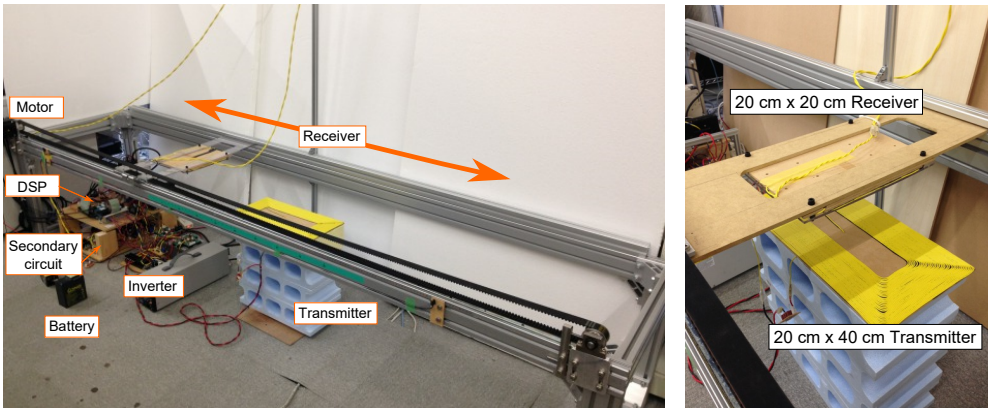

(a) Whole picture of the experimental setup (b) Transmitter and receiver

Figure 11: Experimental setup

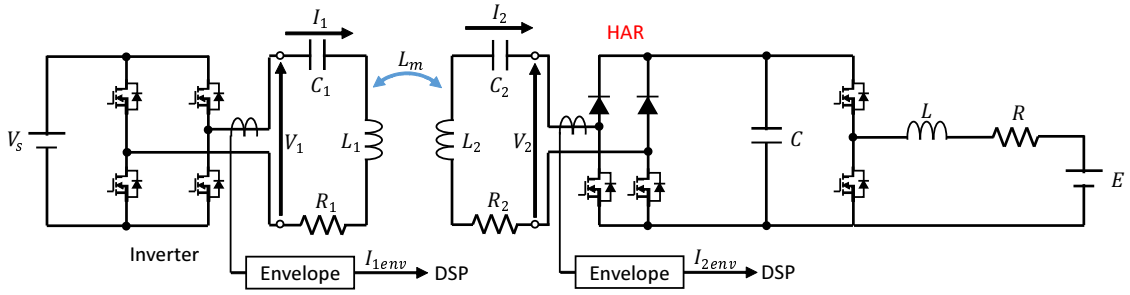

Figure 12: Whole circuit configuration of the experimental setup

3.4.2 How to Determine a Stop Timing of Power Transfer

From (1), current which flows in the secondary coil(RMS value) when a system has a coupling coefficient at which a user want to stop power transfer (k_{off}) is expressed as below.

$$I_{2\_off} = \frac{\omega_0 k_{off}\sqrt{L_1 L_2}V_1 - R_1 V_2}{R_1 R_2 + \omega_0^2 k_{off}^2 L_1 L_2} \tag{3}$$

Accordingly, the secondary circuit can tell a stop timing of power transfer to the primary side at arbitrary k by starting short mode when $I_2 > I_{2\_off}$ is satisfied. Figure 10 shows a flowchart which contains the whole operations explained above.

4 Experiment

In this section, experimental results of the proposed searching method carried out with a experimental setup for DWPT system (Figure 11) are shown.
The whole circuit structure is illustrated in Figure 12. Information of the envelops in the both sides are sent to DSP.
A receiver coil can move above a transmitter coil at arbitrary speed with this experimental setup. The transmitter coil is 20 $\times$ 40 cm, the receiver coil is 20 $\times$ 20 cm, and a vertical gap between the two coil is 10 cm. This experimental setup simulates 1/3 scale model of actual DWPT system. Pseudo-differentiation is used to implement the calculator for differential value of the primary current envelop $\frac{dI_{1env}}{dt}$ and its cut-off frequency is 100 kHz. Parameters and all the threshold values used for the experiment are shown in Table 1. Each current threshold is determined by trial and error.

Table 1: Parameters of the experimental setup

Parameter	Meaning	Value
f_0	Operating frequency	100 kHz
V_s	AC voltage source amplitude	18 V
L_1	Transmitter inductance	417.1 μH
C_1	Transmitter capacitance	6.03 nF
R_1	Transmitter resistance	1.83 Ω
L_2	Receiver inductance	208.5 μH
C_2	Receiver capacitance	12.15 nF
R_2	Receiver resistance	1.28 Ω
T_{search}	Searching period	10 ms
T_{pulse}	Pulse width	0.5 μs
$I_{1env\_th\_on}$	ON threshold current	300 mA
$I_{1env\_diff\_th}$	OFF threshold differentiated primary current envelope	-4000 A/s
k_{off}	OFF threshold coupling coefficient	0.06

4.1 The Primary Voltage and Current

Figure 13 shows the primary voltage and current in search mode (The yellow line is the primary current and blue line is the primary voltage.). In search mode, searching voltage pulse is applied properly and the primary current behaves like that in Figure 6. Figure 14 illustrates the wave forms in transfer mode. The primary inverter is operating properly since the primary voltage is neat square wave in transfer mode.

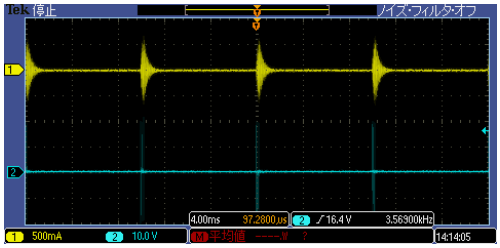

(a) Overall view

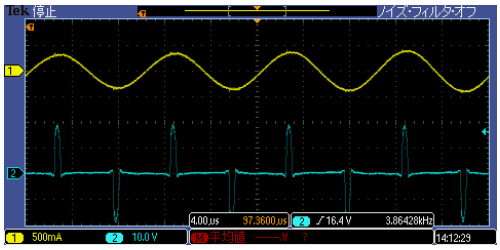

(b) Enlarged view

Figure 13: Primary voltage and current in search mode

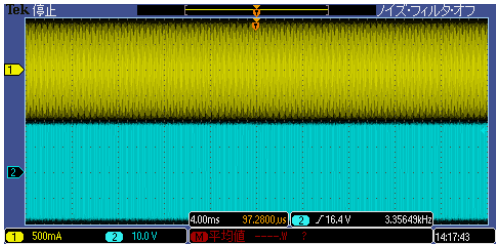

(a) Overall view

(b) Enlarged view

Figure 14: Primary voltage and current in transfer mode

4.2 Dynamic Experiment at 10 km/h

Figure 15 illustrates the experimental results in the case the receiver coil is running at 10 km/h. Figure 15(a) shows the primary current envelop I_{1env}(blue line), the secondary current envelop I_{2env}(green line) and the stopping threshold of the secondary current envelop I_{2env_off}(red line). It can be seen that the power transmission automatically turns ON/OFF even when the receiving coil is running at 10 km/h. Moreover, no large overshoot occurs is the primary current. Figure 15(b) shows their enlarged view and the operations in each period is below.

① Searching pulse application stops as soon as $i_{1\_env} > i_{1env\_th\_on}$ is satisfied

② Searching pulse application continues since $i_{1\_env} > i_{1env\_th\_on}$ is not satisfied

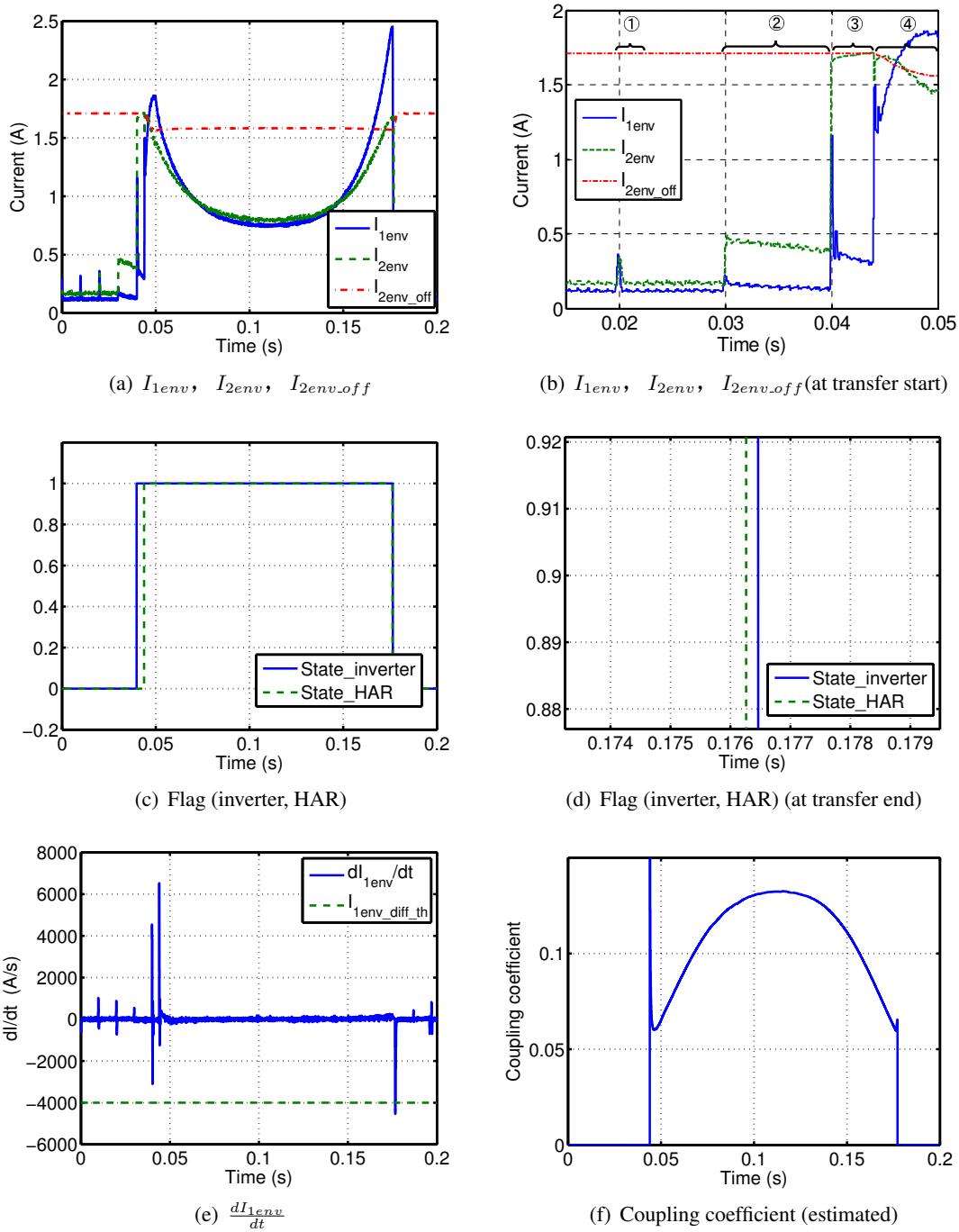

(a) I_{1env}, I_{2env}, I_{2env_off}

(b) I_{1env}, I_{2env}, I_{2env_off}(at transfer start)

(c) Flag (inverter, HAR)

(d) Flag (inverter, HAR) (at transfer end)

(e) $\frac{dI_{1env}}{dt}$

(f) Coupling coefficient (estimated)

Figure 15: Experimental results of the proposed control

③ Power transfer starts after a certain period

④ The secondary side starts receiving power

As described above, the proposed system successfully starts transferring power to the receiver coil moving at 10 km/h.
Figure 15(c) shows inverter's transmitting flag (blue line) and HAR's receiving flag (green line). Transmitting and receiving are conducted when the flags are 1, respectively. Figure 15(d) shows its enlarged view at the end of the transmission. The figure indicates that the receiving flag of HAR gets cleared 0.2 ms before the transmitting flag of the inverter is cleared. This is because $I_{2env} > I_{2env\_off}$ was satisfied in Figure 15(a) and HAR turned into short mode, then the differential value of the primary current

envelop $\frac{dI_{1env}}{dt}$ fell down and $\frac{dI_{1env}}{dt} \leq I_{1env\_diff\_th}$ was satisfied (Figure 15(e)).
Figure 15(f) shows real-time coupling coefficient k between the two coils (estimated value [13]). The figure indicates power was successfully transferred only when the two coils are close enough ($k_{off} > 0.06$).

5 Conclusion

In this paper, the need of vehicle detection in dynamic wireless power transfer system was explained. Moreover, the vehicle detection system which does not use additional sensors was proposed. The proposed method is simple and robust because it uses the primary coil itself as a sensor and just senses the primary current. Finally, the effectiveness of the proposed method has been verified with the experimental results using the experimental setup for DWPT system. In the experiment, the receiving coil runs at 10 km/h in 1/3 scale experimental setup. Therefore, the proposed method should be effective at 30 km/h in real DWPT system. In this paper, the thresholds of current were determined by trial and error. Therefore, a generalized way of threshold determination and the optimization of T_{search} and T_{pulse} are future works.

Acknowledgments

This work was partly supported by JSPS KAKENHI Grant Number 15H02232 and 25709020.

References

[1] J. Shin, S. Shin, Y. Kim, S. Ahn, S. Lee, G. Jung, S. J. Jeon, D. H. Cho, "Design and Implementation of Shaped Magnetic -Resonance-Based Wireless Power Transfer System for Roadway-Powered Moving Electric Vehicles," *IEEE Transactions on Industrial Electronics*, Vol. 61, no.3, pp.1179-1192, 2014.

[2] S. Li, C. C. Mi, "Wireless Power Transfer for Electric Vehicle Applications," *Emerging and Selected Topics in Power Electronics*, Vol. 3, pp.4-17, 2015.

[3] S. Raabe, G. A. Covic, "Practical Design Considerations for Contactless Power Transfer Quadrature Pick-Ups," *IEEE Transactions on Industrial Electronics*, Vol. 60, no.1, pp.400-409, 2013.

[4] W. Li, C. C. Mi, S. Li, "Integrated LCC Compensation Topology for Wireless Charger in Electric and Plug-in Electric Vehicles," *IEEE Transactions on Industrial Electronics*, Vol. 62, pp.4215-4225, 2015.

[5] G. R. Nagendra, L. Chen, G. A. Covic, K. T. Boys, "Detection of EVs on IPT Highways," *IEEE Journal of Emerging and Selected Topics in Power Electronics*, VOL. 2, No. 3, pp.584-597, 2014.

[6] A. Kurs, A. Karalis, R. Moffatt, J. D. Joannopoulos, P. Fisher, and M. Soljacic, "Wireless power transfer via strongly coupled magnetic resonances," *Science*, Vol. 317, no. 5834, pp.83-86, 2007.

[7] Takehiro Imura, Yoichi Hori, "Maximizing Air Gap and Efficiency of Magnetic Resonant Coupling for Wireless Power Transfer Using Equivalent Circuit and Neumann Formula", *IEEE Transactions on Inductrial Electronics*, Vol. 58, No.10, pp.4746-4752, Oct 2011.

[8] D. Kobayashi, T. Imura, Y. Hori, "Real-time coupling coefficient estimation and maximum efficiency control on dynamic wireless power transfer for electric vehicles," *Emerging Technologies: Wireless Power (WoW), 2015 IEEE PELS Workshop on*, pp. 1-6, 2015.

[9] K. Hata, T. Imura, Y. Hori, "Maximum Efficiency Control of Wireless Power Transfer via Magnetic Resonant Coupling Considering Dynamics of DC—DC Converter for Moving Electric Vehicles," *The Applied Power Electronics Conference and Exposition*, pp. 3301-3306, 2015.

[10] Y. D. Ko, Y. J. Jang, "The Optimal System Design of the Online Electric Vehicle Utilizing Wireless Power Transmission Technology", *IEEE Transactions on Intelligent Transportation Systems*, vol. 14, no. 3, pp.1255-1265, 2013.

[11] H. Hao, G. A. Covic, J. T. Boys, “An Approximate Dynamic Model of LCL-T-Based Inductive Power Transfer Power Supplies,” *IEEE transactions on Power Electronics*, Vol. 29, no. 10, 2014.

[12] H. G. Ryu, D. Har,“Wireless Power Transfer for High-precision Position Detection of Railroad Vehicles”, *2015 IEEE Power, Communication and Information Technology Conference (PCITC)*

[13] D. Kobayashi, T. Imura, and Y. Hori, “Real-time Coupling Coefficient Estimation and Maximum Efficiency Control on Dynamic Wireless Power Transfer Using Secondary DC-DC Converter,” *in Proc. 41st Annual Conference of the IEEE Industrial Electronics Society*, pp.4650-4655, 2015.

Authors

Mr. Daita Kobayashi received his B.S. degree in applied physics from Tokyo University of Science in 2014. He is currently working toward a M.S. degree at the Graduate School of Frontier Sciences with the University of Tokyo. His research interests are mainly on wireless power transfer via magnetic resonant couplings.

Mr. Katsuhiro Hata received his B.E. degree in electrical engineering from Ibaraki National College of Technology, Ibaraki, Japan. He received his M.S. degree in Frontier Sciences from The University of Tokyo in September 2015. He is currently working toward a Ph.D. degree at the Graduate School of Engineering with the University of Tokyo. His research interests are mainly on wireless power transfer via magnetic resonant couplings.

Dr. Takehiro Imura received his B.S. degree in electrical and electronics engineering from Sophia University, Tokyo, Japan. He received his M.S. degree and Ph.D. in Electronic Engineering from The University of Tokyo in March 2007 and March 2010 respectively. He is currently a Specially Appointed Associate in the Graduate School of Engineering in the same university.

Dr. Hiroshi Fujimoto received his Ph.D. in electrical engineering from The University of Tokyo in 2001. In 2001, he joined the Department of Electrical Engineering, Nagaoka University of Technology as a research associate. From 2002 to 2003, he was a visiting scholar in the School of Mechanical Engineering, Purdue University. In 2004, he joined the Department of Electrical and Computer Engineering, Yokohama National University as a lecturer and he became an associate professor in 2005. He is currently an associate professor of the University of Tokyo since 2010.

Dr. Yoichi Hori received his Ph.D. in electrical engineering from The University of Tokyo, Japan, 1983, where he became a Professor in 2000. In 2008, he moved to the Department of Advanced Energy, Graduate School of Frontier Sciences. Prof. Hori was the recipient of the Best Paper Award from the IEEE Transactions on Industrial Electronics in 1993, 2001 and 2013 and of the 2000 Best Paper Award from the Institute of Electrical Engineers of Japan (IEEJ). He is the Chairman of the Motor Technology Symposium of the Japan Management Association.